
Spatio-Temporal SwinMAE: A Swin Transformer based Multiscale Representation Learner for Temporal Satellite Imagery

Yohei Nakayama
Degas Ltd.
yohei@degasafrica.com

Jiawei Su
Degas Ltd.
su@degasafrica.com

Abstract

Currently, the foundation models represented by large language models have made dramatic progress and are used in a very wide range of domains including 2D and 3D vision. As one of the important application domains of foundation models, earth observation has attracted attention and various approaches have been developed. When considering earth observation as a single image capture, earth observation imagery can be processed as an image with three or more channels, and when it comes with multiple image captures of different timestamps at one location, the temporal observation can be considered as a set of continuous image resembling video frames or medical SCAN slices. This paper presents Spatio-Temporal SwinMAE (ST-SwinMAE), an architecture which particularly focuses on representation learning for spatio-temporal image processing. Specifically, it uses a hierarchical Masked Auto-encoder (MAE) with Video Swin Transformer blocks. With the architecture, we present a pretrained model named Degas 100M as a geospatial foundation model. Also, we propose an approach for transfer learning with Degas 100M, which both pretrained encoder and decoder of MAE are utilized with skip connections added between them to achieve multi-scale information communication, forms an architecture named Spatio-Temporal SwinUNet (ST-SwinUNet). Our approach shows significant improvements of performance over existing state-of-the-art of foundation models. Specifically, for transfer learning of the land cover downstream task on the PhLEO Bench dataset, it shows 10.4% higher accuracy compared with other geospatial foundation models on average.

1 Introduction

Foundation models (FMs), represented by large language models (LLMs), have undergone rapid development and are used in a variety of applications. The basic concept of FMs is to train backbone models by conducting representation learning of data features on a broad spectrum of generalized and unlabeled data, and use them as a starting point to develop deep learning models for a wide variety of general tasks more quickly and cost-effectively [1]. Recently, Convolutional Neural Networks (CNNs) have been replaced by Vision Transformer (ViT) on different vision understanding tasks [2, 3]. ViT globally models spatial relationships on non-overlapping image patches with the standard Transformer encoder and the evaluation shows that a pure Transformer applied directly to sequences of image patches can have good performances on different downstream tasks without any reliance on CNNs. Consequently, many researchers in geo-spatial domain are inspired to develop ViT-based FMs and various research and studies have been published.

In the field of earth observation and remote sensing, various satellite constellations have been realized, both commercial and non-commercial, and satellite data has become more accessible. A long-standing

problem in developing deep learning models for earth observation data has been the difficulty of creating datasets with large numbers of annotations. Therefore, applying n-shot training to tasks via the FMs is considered an important approach in this field. Until now, various FMs have been created through self-supervised learning on ViT-based models and applied to downstream tasks such as scene classification, land cover segmentation, cloud gap imputation, super resolution, and so on.

However, existing FMs share several representative limitations. First, for most pretrained FMs, only the encoder is preserved for transfer learning, with an encoder-bottleneck-head structure. Since the bottleneck is always of low complexity with a single-stream structure, the information that can be stored and forwarded through the neck is highly abstracted and limited, in other words the low-level spatial information can be significantly diluted by going through the neck therefore the output of the head will be solely dominated by the outputs of decoder. Second, despite good performances, existing FMs failed to extend to more generalized scenarios. Most FMs focus on handling spatial data while neglecting the temporal dimension, which is an important nature of geo-spatial data. This limited the further extension and enhancement of existing FMs with temporal information.

In this paper, we present an architecture for spatio-temporal geo-spatial FM and an efficient transfer learning approach specifically for images-to-images tasks(e.g., segmentation). We are motivated by, therefore fuse and extend advanced features of MAE[4], Swin Transformer[3] and SwinUNet[5]. First, self-supervised training using MAE is conducted with a Swin Transformer backbone. MAE has been proved to be an efficient and effective model for learning general feature representation on unlabeled data. The shifted-windows and patch-merging originated from Swin Transformer are extended to 3-dimensional for handling temporal geo-spatial data, in order to add inductive bias for spatial locality, hierarchy and translation invariance to 3-dimensional ViT backbone. Then transfer learning is conducted using both pretrained encoder and decoder where the skip connections are added to enable the communication from encoder to decoder for restoring the spatial resolution of the feature maps, allowing forwarding low-level features from encoder layers to decoders' for local-global semantic feature learning.

Our contributions can be summarized as:

1. We generalize the SwinMAE and SwinUNet through the temporal axis by extending the shifted-windows, patch-merging and patch-expanding to 3-dimensional, namely ST-SwinMAE and ST-SwinUNet.
2. We propose a novel learning scheme for 3-dimensional geospatial information. Specifically, we pretrain a ST-SwinMAE, preserve both encoder and decoder, add UNet-like skip connections from encoder to decoder blocks for forwarding low-level features, results in forming ST-SwinUNet structure, and conduct transfer learning for downstream tasks by adding task-specific heads.
3. We pretrained our model on SSL4EO-S12 [6], which is a large-scale earth observation dataset for self-supervised learning, and evaluate the Degas 100M on several benchmark datasets.

The rest of this paper is organized as follows. Section II describes the research background of this paper. Section III introduces our proposed method. Section IV presents the relevant experiments and experimental results. Section V summarizes the paper and discusses future potential extensions.

2 Background

Geo-spatial Representation Learning Remote sensing can constantly provide a vast supply of data(e.g.,Satellite Imagery) which facilitates machine learning[7, 8]. However, the lack of annotations poses challenges for supervised training of deep learning models. This induces the necessity of self-supervised learning, which is about learning an universal underlying representation of data features from vast amounts of unlabeled samples that is expected to generalize well to different downstream tasks [9]. To this end, self-supervised learning [10] has been shown as an effective approach for processing remote sensing data [10, 11, 12, 13] by either conducting the learning (e.g., contrastive learning [14, 15]) in a similar way to typical vision tasks or by adding domain-specific knowledge (e.g., carefully crafted pre-text tasks or priors) to the original learning pipeline [16, 17, 18].

In particular, several proposed FMs for earth science applications have shown outstanding performance on different downstream tasks [19]. For example, SatMAE [20] is a Masked Auto-Encoder (MAE) [4] trained on temporal and multi-spectral information. Its pretrained encoder can be then utilized for fine-tuning on multiple tasks such as land cover classification, multi-label classification and building segmentation. MAE defines an input image before and after reconstruction as a positive pair and the pretext task as reconstructing masked patches of the input. It uses ViT [2] encoder as its backbone for representation learning. However, being different from CNNs, since ViT lacks the inductive bias such as locality and translation equivariance, it has been shown as a data hungry model which in most cases requires pretraining on large-scale datasets [21]. Other ViT-based FMs are also proposed. For example Prithvi [19] is a ViT encoder pretrained on temporal satellite images and PRESTO [22] is trained on time-series data.

Multi-scale A notable feature of remote sensing data is that scale of the objects may vary depending on satellites. Extension based on SatMAE, such as Scale-MAE [23] and ConvMAE [24] aim to add local inductive bias and hierarchical representation features to the original MAE for extracting multi-scale feature mappings.

Specifically, Scale-MAE introduced a domain-specific embedding of position and scale information for RGB images as well as a Laplacian pyramid based decoder for learning multi-scale representation. ConvMAE has an encoder that progressively embeds the input image into multi-scale patch tokens. The encoder consists of convolution and transformer blocks, which are for encoding local features from high-resolution tokens at early stages and aggregating global features at later stages respectively. Therefore both local and global semantic information at different scales can be extracted. In addition, SatMAE++[25] proposed a modified relative positional embedding for multi-spectral imagery. The loss of image reconstructing is calculated on three different sizes of inputs for encouraging learning features of different scales. SwinUNet[5] combines swin transformer with skip connections such that the high-level features extracted from decoder are fused with multi-scale low-level features from encoder via skip connections to complement the loss of spatial information caused by down-sampling.

To understand how multi-scale features can help with learning a better feature representation, it is worth to mention a comparison of performance on different downstream tasks where the simple UNet outperforms other pretrained FMs with more advanced structures and training strategies [26]. It is considered that since these pretrained FMs use a narrow, single stream bottleneck for forwarding information to the headers, the amount of information that can be stored in and past through the bottleneck is limited. In other words only the high-level features extracted from few layers before the bottleneck can be preserved which poses a challenge of pretraining without multi-scale features. UNet[27] and SwinUNet[5] uses skip connections to mitigate this problem by bypassing the bottleneck and forward low-level features directly to the decoder, providing rich multi-scale information to train a better self-supervised model.

Locality For processing 2-dimensional images, ViT follows the same procedure of handling word vectors defined in original transformer, which is simply conducting global attention computation on all patches therefore 1) it can hardly handle high resolution images with small size of patches and pixel-level tasks such as semantic segmentation due to heavy cost of quadratically scaling attention computation with the sequence length and 2) not be able to well recognize different object entities due to large variations in the scale of objects in images. Therefore Swin Transformer [28] is proposed for tackling these problems in a hierarchical way. Specifically, patch-merging(similar to pooling operation) is introduced for extracting features of different scales hierarchically. On the other hand, the novel shifted-windows mechanism(similar to strided convolution) enables the exchange of information between each separate window(a group of local patches). The attention computation can now be merely conducted inside each window which significantly reduced the computation cost.

SwinMAE [29] is a MAE model using Swin Transformer as backbone for medical image processing. Despite the performance, the lack of convolution-like inductive biases challenges the training of ViT with excessive demands of data, computing, and sophisticated tuning of many hyperparameters. Combining Swin Transformer with MAE introduces inductive biases to the model therefore mitigated these problems compared with original MAE [21].

Temporal Compare to typical vision tasks, another critical unique to remote sensing data is satellite revisiting therefore for a same location on earth, repeated snapshots can be captured to form temporal

data[30]. Adding this extra temporal dimension can be seen as a domain-specific data augmentation which can facilitate many downstream tasks by providing additional (temporal) information. Repeated snapshots on the same location can be also seen as (temporal) positive pairs for constructing pre-text task for contrastive learning. According to the impressed performance of ViT and its variants on 2-dimensional image processing [31, 32, 33, 34], it is natural to extend the evaluation to 3-dimensional temporal images. ViViT [35] examined two types of embeddings and four factorized designs of spatial and temporal attention for the pretrained ViT model on video data. The experiment shows that the combination of 3-dimensional tubelet embedding and spatio-temporal attention gives the best performance. Video Swin Transformer [28] extended 2-dimensional Swin Transformer by introducing 3-dimensional patch merging and shifted windows mechanism for handling continuous video frames. It extends the scope of local attention computation from only the spatial to the spatio-temporal domain. Same as ViViT, Video Swin Transformer also uses tubelet embedding with spatio-temporal attention. In this paper we follow this setting. VideoMAE [36] is proposed by extending the original 2-dimensional tubelet masking and patchifying to 3-dimensional.

However, the performance of 3-dimensional ViTs is based on the assumption of equally-spaced video frames in the temporal dimension, whereas in the case of satellite data, the temporal irregularity and discontinuity in temporal images of a location might make the performance of these model no longer promising, which makes the further evaluation non-trivial. Hence we aim to fill this gap in this paper by conducting a comprehensive evaluation on remote sensing data with our proposed model. Specifically, our proposal addresses the following problems: 1) reduce the loss of spatial information caused by down-sampling using skip connections. 2) mitigate data hungry, high computational cost problem, achieve local-global multi-scale feature representation learning by adding CNN-like inductive bias for spatial locality, hierarchy and translation invariance. 3) extend existing 2-dimensional model for 3-dimensional temporal remote sensing data processing.

3 Methodology

3.1 Pretraining

3.1.1 Dataset

SSL4EO-S12 [6] is a large-scale earth observation dataset for self-supervised learning. There are 250K locations on earth that have been sampled, each providing Sentinel-2 L1C (top-of-atmosphere multi-spectral), Sentinel-2 L2A (surface reflectance multi-spectral), and Sentinel-1 GRD images with four snapshots from different seasons, resulting 3 million 2640m×2640m unlabeled patches in total. The image patches are further pre-processed to guarantee reasonable global coverage. Overlapping patches and Sentinel-2 tiles with a cloud coverage higher than 10% are removed. Several representative SSL algorithms such as MoCo [10], DINO [37], MAE [4] and data2vec [38] are evaluated on SSL4EO-S12 on three different downstream tasks: scene classification, semantic segmentation and change detection.

In this paper, we use the compressed version of Sentinel-2 L1C dataset. The compressed dataset is provided in normalized 8-bit GeoTiff format. Sentinel-2 L1C provides observation data of 13 channels but we only use 6 channels (B2, B3, B4, B8A, B11, B12) for training. We randomly selects the first season for each patch and extracts data for the following two seasons as input. The pixels are also cropped to 224×224, resulting in a final sample size of 3×224×224×6.

3.1.2 Model Architecture

First, we clarify the difference between our work and two related works: SwinMAE and SwinUNet. SwinMAE follows a self-supervised training pipeline. SwinUNet is a UNet-like model trained with supervised learning. In addition, both works are for processing spatial medical image processing. On the other side, our work trains a MAE with Swin Transformer blocks with self-supervised learning, keeps both pretrained encoder and decoder, then adds UNet-like skip-connections for transfer learning. Besides, we test our model on temporal geospatial data.

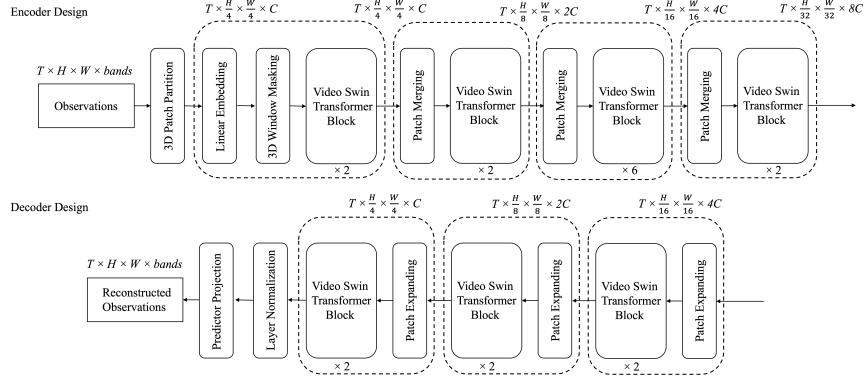


Figure 1: The architecture of ST-SwinMAE.

Specifically, we extend SwinMAE [29] to handle the spatio-temporal information, namely ST-SwinMAE. The encoder and decoder design of ST-SwinMAE is shown in Figure 1. The satellite observations are inputs defined to be of size $T \times H \times W \times \text{bands}$ where T is the time dimension, H and W are the spatial size.

In the encoder, raw inputs are transformed into embedding sequences and split into non-overlapping patches. Similar to the Video Swin Transformer [28], each 3-dimensional patch of size $1 \times 4 \times 4 \times \text{bands}$ is treated as a token. Thus, the 3-dimensional patch partitioning layer obtains $T \times H/4 \times W/4$ 3-dimensional tokens. A linear embedding layer is then applied to project the features of each token to an arbitrary dimension denoted by C . The tokens are then continued into the subsequent four Video Swin Transformer stages in total, with no patch merging layer after the last block, consistent with the encoder of SwinUNet [5] used in the downstream task. The patch merging layer concatenates the features of each group of $1 \times 2 \times 2$ spatially neighboring patches and applies a linear projection on concatenated features to reduce their feature dimension to half.

As a masking strategy, we applied window masking layer [29] to each spatial slice, in which the minimum unit of the random mask operation forms a window containing multiple patches. For each slice, mask positions are randomly selected, which is equivalent to the method named random masking in VideoMAE [36]. Each window masking layer does not remove the mask tokens, but directly and uniformly replaces them with a learnable vector, thus leaving the number of tokens unchanged.

The decoder consists of Video Swin Transformer blocks and patch expanding layers. A patch expanding layer is a reverse operation of patch merging which performs up-sampling for replacing convolution or interpolation. Specifically first a linear projection is applied on the input to double the feature dimension C . Then, the spatial size expands such that the resolution of the input features to $2 \times$ the input resolution and the feature dimension C reduces to quarter of the input dimension. With a projection layer, the feature maps are reconstructed as 3-dimensional multi-spectral images with the same shape to inputs. Note that both patch merging and expanding do not operate along the temporal dimension.

3.1.3 Training Settings

With the definition of the architecture, we experimented with Swin-Base backbones to have of model size and computation complexity similar to ViT-Base. Here in after we call the pretrained model as Degas 100M. Degas 100M can easily scale, for example, with applying Swin-T, Swin-S and Swin-L backbones, which are versions of about $0.25 \times$, $0.5 \times$ and $2 \times$ the model size and computational complexity, respectively. The window size is set to $M = 7$ by default. The query dimension of each head is $d = 32$, and the expansion layer of each MLP is $\alpha = 4$, for all experiments. We use AdamW optimizer with $\beta_1 = 0.9$, $\beta_2 = 0.999$, batch size of 1536, one-cycle cosine learning rate scheduler, with a maximum learning rate of $1e-5$. All the pretraining runs are conducted using 64 NVIDIA A100 GPUs.

3.2 Transfer Learning

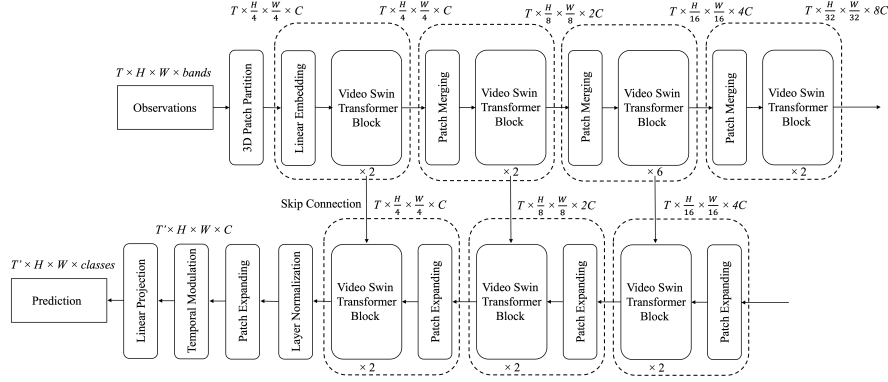


Figure 2: The architecture of ST-SwinUNet.

Transfer learning is performed to verify whether the trained model can be more efficiently applied to downstream tasks. Downstream tasks in remote sensing can be broadly divided into classification and segmentation, but we focus on segmentation in particular and propose an architecture for transfer learning as shown in Figure 2. This structure can also be considered a 3-dimensional extended version of SwinUNet, namely ST-SwinUNet.

Specifically for transfer learning, the encoder part keeps the same except that the window mask module has been removed while the predictor projection layer for reconstructing is replaced with a temporal segmentation head which consists of a patch expanding layer, a temporal modulation layer and a project layer. The feature map from the layer-normalization layer is up-sized to $T \times H \times W \times C/4$ through patch expanding, and converted to a time frame size according to the task using the Temporal Modulation module. After that, the Linear Projection module converts it to a shape of $T' \times H \times W \times \text{Class}$ and output it as segmentation results. The Temporal Modulation module is a 3-dimensional CNN that adjusts the kernel size to change the output time frame size. At last, skip connections are introduced to link the Video Swin Transformer blocks in the encoder and decoder with the same scale. For classification tasks, we use the output from the encoder.

Note that unlike original MAE, which only preserves encoder, we keep both pretrained encoder and decoder for transfer learning due to the usage of skip connections and corresponding patch-expanding layers for forwarding multi-scale features. Specifically, the skip connections are for fusing the multi-scale low-level features from the encoder with the up-sampled high-level features, which can reduce the loss of spatial information caused by down-sampling during fine-tuning.

4 Experiments and Discussion

4.1 Pretraining

The pretraining is terminated with a MSE loss value of $2.65e-4$. An Example of re-constructed satellite imagery is shown in Figure 3. The original, masked and reconstructed satellite imagery for three seasons is displayed respectively. It can be seen that the reconstruction was performed with high quality. In particular, it is worth mentioning that the clouds that only occur at snapshot T_0 are also successfully reconstructed indicating that the reconstruction has been actually benefited with the spatial dimension complementation instead of temporal dimension complementation due to the absence of clouds in other snapshots (seasons).

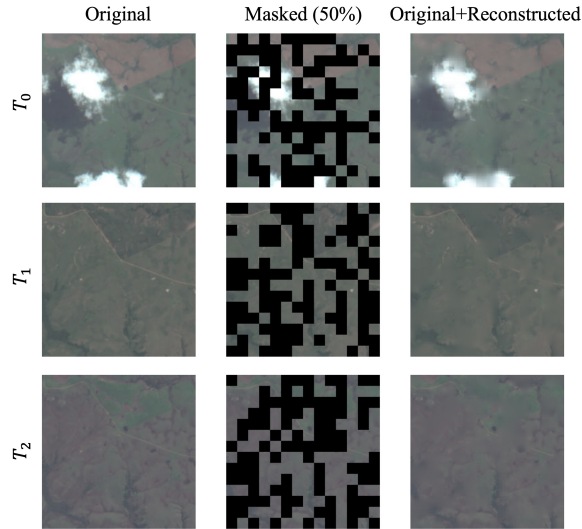


Figure 3: An example of re-constructed satellite imagery during pretraining. Only RGB bands are shown here for visualization.

4.2 Transfer Learning

To evaluate the pretrained model, we perform transfer learning and verified its accuracy on downstream tasks. In this paper, we evaluate on 2 datasets: PhilEO Bench dataset [26] and the dataset proposed with Prithvi [19].

4.2.1 PhilEO Bench Dataset

PhilEO Bench is a newly introduced global dataset with an aim to benchmark universality of geospatial foundation models. At this point, a benchmark dataset for 3 different downstream tasks is provided on the framework: land cover, buildings and roads. Sentinel-2 images sampled from geographically diverse 14 regions around the globe are labeled for the 3 downstream tasks which forms a 400 GB global dataset. In this paper, we choose the land cover and building dataset and evaluate the performance of our model to the image-to-image downstream tasks.

Land Cover Land cover labels have 11 classes which are taken from ESA World Cover. In Figure 4, we compare the land cover segmentation accuracy of foundation models (SeCo [11], SatMAE [20] and Prithvi [19]) provided on the PhilEO Bench platform versus the training dataset size.

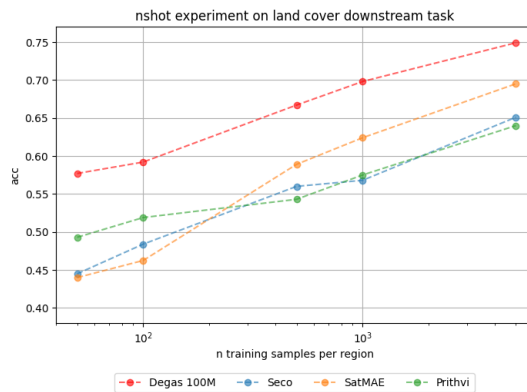


Figure 4: PhilEO Bench land cover segmentation results.

Our proposed Degas 100M achieves better results compared to the FMs (SeCo, SatMAE and Prithvi). Specifically, Degas 100M shows 10.4% higher accuracy compared with other FMs on average. It is worth mentioning that the Geo-Aware UNet provided on Phileo Bench [26] shows similar results as our model on this task. Geo-Aware UNet is a mixture of classification and regression model pretrained with supervised-learning for predicting the co-ordinates, capture time and majority kg class of Sentinel-2 patches. Considering the fact that our FM without pretraining outperforms UNet, we consider the possible reasons can be as (1) Geo-aware UNet is trained with supervised learning with unambiguous supervised annotations which is easier to converge. (2) Geo-aware UNet directly learns to predict semantic geospatial information while our model learns indirect pixel-level features. This can be potentially addressed by adding more geo-aware information such as embedding to our framework. We leave the explore of the above aspects as future works.

Building Density Building labels are expressed as a number of squared meters of roads in a given pixel. The values are between 0 and 100, and for a resolution of 10m, this reflect the percentage of coverage.

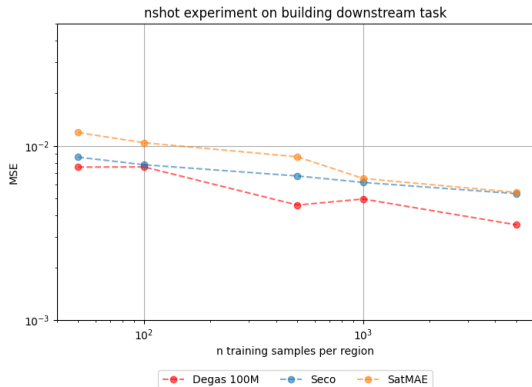


Figure 5: Phileo Bench building density prediction results.

For the purpose of fair evaluation, we showed results of the building density task only for models with trained on 10m resolution data. The models which use higher resolution data as input skew the results in their favour [26]. Degas 100M also showed better results compared to FMs.

4.2.2 Flood Mapping, Wildfire Scar Mapping and Multi-Temporal Crop Segmentation Dataset

We applied Degas 100M to 3 downstream tasks: Flood Mapping, Wildfire Scar Mapping and Multi-Temporal Crop Segmentation, which are proposed together with Prithvi [19].

Flood Mapping As a flood mapping dataset, we use Sen1Flood11 which provides a surface water dataset consists of 4831 512×512 chips spans all 14 biomes, 357 ecoregions, and 6 continents of the world across 11 flood events.

Table 1: Sen1Floods11 [39] flood segmentation results.

Method	IoU (water)	mIoU (both classes)	mAcc (both classes)
Baseline [39]	24.21	–	–
ViT-base [2]	67.58	81.06	88.82
Swin [3]	79.43	87.48	90.63
Swin (pretrained on ADE20K) [3]	80.58	87.98	92.02
Prithvi (pretrained) [19]	82.99	90.16	94.60
Degas 100M (pretrained)	84.47	91.12	96.23

Table 1 shows a comparison of performance in flood mapping dataset. Our Degas 100M shows the best score in all metrics of IoU, mIoU, and mAcc. Additionally, the performance has significantly increased compared to regular Swin Transformer, indicating the effectiveness of architecture and pretraining of our model.

Wildfire Scar Mapping Wildfire scar dataset is created gathering data from the Monitoring Trends in Burn Severity (MTBS) historical fire database. Wildfire data has been collected from 2018 to 2021, in line with the availability period of HLS, and a 512×512 pixel HLS image centered on the wildfire scar forms one sample. In total, 805 scenes are available for training and validation.

Table 2: Wildfire scars segmentation results.

Method	IoU (fire scar)	mIoU (both classes)	mAcc (both classes)
U-Net (DeepLabV3) [40]	71.01	83.55	87.98
ViT-base [2]	69.04	82.20	90.14
Prithvi (pretrained)	73.62	84.84	92.48
Degas 100M (pretrained)	74.92	85.96	93.44

Table 2 shows that Degas 100M achieves state-of-the-art in the wildfire scar segmentation task as well. In this result, the performance of Degas 100M is better than UNet, which also indicates the effectiveness of our approach.

Multi-Temporal Crop Segmentation Sentinel observations of the Contiguous United States was gathered for 2022 together with the crop type labels from USDA’s Crop Data Layer (CDL). Each input sample consists of three temporal snapshots of Sentinel with the size of a 224 × 224 pixel region and a spatial resolution of 30 m.

Table 3: Multi-temporal crop type segmentation results.

Method	mIoU	mAcc
U-Net (DeepLabV3) [40]	0.420	61.91
Prithvi (pretrained)	0.426	64.06
Degas 100M (pretrained)	0.466	67.68

The results in table 3 show that our pretrained model achieves better performance both in mIoU and mAcc compared to U-Net and Prithvi. In particular, in mIoU, the results of U-Net and Prithvi are 0.420 and 0.426, respectively, while the result of Degas FM is 0.466, which shows a significant difference.

5 Conclusion

In this paper, we focused on the primary features of earth observation, namely multi-scale, locality and temporal. To address this focus, we introduced novel architectures based on the Swin Transformer for pretraining and transfer learning of geospatial foundation model. Additionally, we assessed the effectiveness of our proposed approach through verifying application performance of the pretrained model across downstream tasks. Our approach demonstrated superior performance compared to alternative foundation models, notably surpassing the current state-of-the-art. On the other hand, it has been shown that adding multi-modal Geo-Aware information, such as Geo-Aware embedding(timestamp of a satellite image)[20] and pre-text[41] is an effective approach of improving self-supervised pretraining. We also consider to fuse these multi-modal domain-specific knowledge to our model as future works. Our proposal is an universal 3-dimensional image processing approach that can be easily generalized to other vision domains such as continues video frame and 3-dimensional medical image processing. Also, we believe that the foundation model introduced in this study will facilitate its adoption across diverse domains, including agriculture, urban planning and climate change research.

References

- [1] Rishi Bommasani, Drew A Hudson, Ehsan Adeli, Russ Altman, Simran Arora, Sydney von Arx, Michael S Bernstein, Jeannette Bohg, Antoine Bosselut, Emma Brunskill, et al. On the opportunities and risks of foundation models. *arXiv preprint arXiv:2108.07258*, 2021.
- [2] Alexey Dosovitskiy, Lucas Beyer, Alexander Kolesnikov, Dirk Weissenborn, Xiaohua Zhai, Thomas Unterthiner, Mostafa Dehghani, Matthias Minderer, Georg Heigold, Sylvain Gelly, et al. An image is worth 16x16 words: Transformers for image recognition at scale. *arXiv preprint arXiv:2010.11929*, 2020.
- [3] Ze Liu, Yutong Lin, Yue Cao, Han Hu, Yixuan Wei, Zheng Zhang, Stephen Lin, and Baining Guo. Swin transformer: Hierarchical vision transformer using shifted windows. In *Proceedings of the IEEE/CVF international conference on computer vision*, pages 10012–10022, 2021.
- [4] Kaiming He, Xinlei Chen, Saining Xie, Yanghao Li, Piotr Dollár, and Ross Girshick. Masked autoencoders are scalable vision learners. In *Proceedings of the IEEE/CVF conference on computer vision and pattern recognition*, pages 16000–16009, 2022.
- [5] Hu Cao, Yueyue Wang, Joy Chen, Dongsheng Jiang, Xiaopeng Zhang, Qi Tian, and Manning Wang. Swin-unet: Unet-like pure transformer for medical image segmentation. In *European conference on computer vision*, pages 205–218. Springer, 2022.
- [6] Yi Wang, Nassim Ait Ali Braham, Zhitong Xiong, Chenying Liu, Conrad M Albrecht, and Xiao Xiang Zhu. Ssl4eo-s12: A large-scale multimodal, multitemporal dataset for self-supervised learning in earth observation [software and data sets]. *IEEE Geoscience and Remote Sensing Magazine*, 11(3):98–106, 2023.
- [7] Neal Jean, Marshall Burke, Michael Xie, W Matthew Davis, David B Lobell, and Stefano Ermon. Combining satellite imagery and machine learning to predict poverty. *Science*, 353(6301):790–794, 2016.
- [8] Burak Uzcent, Evan Sheehan, Chenlin Meng, Zhongyi Tang, Marshall Burke, David Lobell, and Stefano Ermon. Learning to interpret satellite images using wikipedia. In *Proceedings of the Twenty-Eighth International Joint Conference on Artificial Intelligence*, 2019.
- [9] Yi Wang, Conrad M Albrecht, Nassim Ait Ali Braham, Lichao Mou, and Xiao Xiang Zhu. Self-supervised learning in remote sensing: A review. *IEEE Geoscience and Remote Sensing Magazine*, 10(4):213–247, 2022.
- [10] Kaiming He, Haoqi Fan, Yuxin Wu, Saining Xie, and Ross Girshick. Momentum contrast for unsupervised visual representation learning. In *Proceedings of the IEEE/CVF conference on computer vision and pattern recognition*, pages 9729–9738, 2020.
- [11] Oscar Manas, Alexandre Lacoste, Xavier Giró-i Nieto, David Vazquez, and Pau Rodriguez. Seasonal contrast: Unsupervised pre-training from uncurated remote sensing data. In *Proceedings of the IEEE/CVF International Conference on Computer Vision*, pages 9414–9423, 2021.
- [12] AM Swope, XH Rudelis, and KT Story. Representation learning for remote sensing: An unsupervised sensor fusion approach. arxiv 2021. *arXiv preprint arXiv:2108.05094*, 2021.
- [13] Michail Tarasiou and Stefanos Zafeiriou. Embedding earth: Self-supervised contrastive pre-training for dense land cover classification. *arXiv preprint arXiv:2203.06041*, 2022.
- [14] Ishan Misra and Laurens van der Maaten. Self-supervised learning of pretext-invariant representations. In *Proceedings of the IEEE/CVF conference on computer vision and pattern recognition*, pages 6707–6717, 2020.
- [15] Ting Chen, Simon Kornblith, Mohammad Norouzi, and Geoffrey Hinton. A simple framework for contrastive learning of visual representations. In *International conference on machine learning*, pages 1597–1607. PMLR, 2020.
- [16] Grace Chu, Brian Potetz, Weijun Wang, Andrew Howard, Yang Song, Fernando Brucher, Thomas Leung, and Hartwig Adam. Geo-aware networks for fine-grained recognition. In *Proceedings of the IEEE/CVF International Conference on Computer Vision Workshops*, pages 0–0, 2019.
- [17] Oisín Mac Aodha, Elijah Cole, and Pietro Perona. Presence-only geographical priors for fine-grained image classification. In *Proceedings of the IEEE/CVF International Conference on Computer Vision*, pages 9596–9606, 2019.

- [18] Eric Muller-Budack, Kader Pustu-Iren, and Ralph Ewerth. Geolocation estimation of photos using a hierarchical model and scene classification. In *Proceedings of the European conference on computer vision (ECCV)*, pages 563–579, 2018.
- [19] Johannes Jakubik, Sujit Roy, CE Phillips, Paolo Fraccaro, Denys Godwin, Bianca Zadrozny, Daniela Szwarzman, Carlos Gomes, Gabby Nyirjesy, Blair Edwards, et al. Foundation models for generalist geospatial artificial intelligence. *arXiv preprint arXiv:2310.18660*, 2023.
- [20] Yezhen Cong, Samar Khanna, Chenlin Meng, Patrick Liu, Erik Rozi, Yutong He, Marshall Burke, David Lobell, and Stefano Ermon. Satmae: Pre-training transformers for temporal and multi-spectral satellite imagery. *Advances in Neural Information Processing Systems*, 35:197–211, 2022.
- [21] Xiangning Chen, Cho-Jui Hsieh, and Boqing Gong. When vision transformers outperform resnets without pre-training or strong data augmentations. *arXiv preprint arXiv:2106.01548*, 2021.
- [22] Gabriel Tseng, Ruben Cartuyvels, Ivan Zvonkov, Mirali Purohit, David Rolnick, and Hannah Kerner. Lightweight, pre-trained transformers for remote sensing timeseries. *arXiv preprint arXiv:2304.14065*, 2023.
- [23] Colorado J Reed, Ritwik Gupta, Shufan Li, Sarah Brockman, Christopher Funk, Brian Clipp, Kurt Keutzer, Salvatore Candido, Matt Uyttendaele, and Trevor Darrell. Scale-mae: A scale-aware masked autoencoder for multiscale geospatial representation learning. In *Proceedings of the IEEE/CVF International Conference on Computer Vision*, pages 4088–4099, 2023.
- [24] P Gao, T Ma, H Li, Z Lin, J Dai, and Y Qiao. Convmae: Masked convolution meets masked autoencoders.” arxiv, may 19, 2022. doi: 10.48550. *arXiv preprint arXiv:2205.03892*, 2022.
- [25] Mubashir Noman, Muzammal Naseer, Hisham Cholakkal, Rao Muhammad Anwar, Salman Khan, and Fahad Shahbaz Khan. Rethinking transformers pre-training for multi-spectral satellite imagery. *arXiv preprint arXiv:2403.05419*, 2024.
- [26] Casper Fibaek, Luke Camilleri, Andreas Luyts, Nikolaos Dionelis, and Bertrand Le Saux. Phileo bench: Evaluating geo-spatial foundation models. *arXiv preprint arXiv:2401.04464*, 2024.
- [27] Olaf Ronneberger, Philipp Fischer, and Thomas Brox. U-net: Convolutional networks for biomedical image segmentation. In *Medical image computing and computer-assisted intervention—MICCAI 2015: 18th international conference, Munich, Germany, October 5-9, 2015, proceedings, part III 18*, pages 234–241. Springer, 2015.
- [28] Ze Liu, Jia Ning, Yue Cao, Yixuan Wei, Zheng Zhang, Stephen Lin, and Han Hu. Video swin transformer. In *Proceedings of the IEEE/CVF conference on computer vision and pattern recognition*, pages 3202–3211, 2022.
- [29] Yin Dai, Fayu Liu, Weibing Chen, Yue Liu, Lifu Shi, Sheng Liu, Yuhang Zhou, et al. Swin mae: masked autoencoders for small datasets. *Computers in biology and medicine*, 161:107037, 2023.
- [30] Matthias Drusch, Umberto Del Bello, Sébastien Carlier, Olivier Colin, Veronica Fernandez, Ferran Gascon, Bianca Hoersch, Claudia Isola, Paolo Laberinti, Philippe Martimort, et al. Sentinel-2: Esa’s optical high-resolution mission for gmes operational services. *Remote sensing of Environment*, 120:25–36, 2012.
- [31] Wenhai Wang, Enze Xie, Xiang Li, Deng-Ping Fan, Kaitao Song, Ding Liang, Tong Lu, Ping Luo, and Ling Shao. Pyramid vision transformer: A versatile backbone for dense prediction without convolutions. In *Proceedings of the IEEE/CVF international conference on computer vision*, pages 568–578, 2021.
- [32] Chenglin Yang, Yilin Wang, Jianming Zhang, He Zhang, Zijun Wei, Zhe Lin, and Alan Yuille. Lite vision transformer with enhanced self-attention. In *Proceedings of the IEEE/CVF Conference on Computer Vision and Pattern Recognition*, pages 11998–12008, 2022.
- [33] Sachin Mehta and Mohammad Rastegari. Mobilevit: light-weight, general-purpose, and mobile-friendly vision transformer. *arXiv preprint arXiv:2110.02178*, 2021.
- [34] Daquan Zhou, Bingyi Kang, Xiaojie Jin, Linjie Yang, Xiaochen Lian, Zihang Jiang, Qibin Hou, and Jiashi Feng. Deepvit: Towards deeper vision transformer. *arXiv preprint arXiv:2103.11886*, 2021.

- [35] Anurag Arnab, Mostafa Dehghani, Georg Heigold, Chen Sun, Mario Lučić, and Cordelia Schmid. Vivit: A video vision transformer. In *Proceedings of the IEEE/CVF international conference on computer vision*, pages 6836–6846, 2021.
- [36] Zhan Tong, Yibing Song, Jue Wang, and Limin Wang. Videomae: Masked autoencoders are data-efficient learners for self-supervised video pre-training. *Advances in neural information processing systems*, 35:10078–10093, 2022.
- [37] Mathilde Caron, Hugo Touvron, Ishan Misra, Hervé Jégou, Julien Mairal, Piotr Bojanowski, and Armand Joulin. Emerging properties in self-supervised vision transformers. In *Proceedings of the IEEE/CVF international conference on computer vision*, pages 9650–9660, 2021.
- [38] Alexei Baevski, Wei-Ning Hsu, Qiantong Xu, Arun Babu, Jiatao Gu, and Michael Auli. Data2vec: A general framework for self-supervised learning in speech, vision and language. In *International Conference on Machine Learning*, pages 1298–1312. PMLR, 2022.
- [39] Derrick Bonafilia, Beth Tellman, Tyler Anderson, and Erica Issenberg. Sen1floods11: A georeferenced dataset to train and test deep learning flood algorithms for sentinel-1. In *Proceedings of the IEEE/CVF Conference on Computer Vision and Pattern Recognition Workshops*, pages 210–211, 2020.
- [40] Liang-Chieh Chen, George Papandreou, Florian Schroff, and Hartwig Adam. Rethinking atrous convolution for semantic image segmentation. *arXiv preprint arXiv:1706.05587*, 2017.
- [41] Kumar Ayush, Burak Uzkent, Chenlin Meng, Kumar Tanmay, Marshall Burke, David Lobell, and Stefano Ermon. Geography-aware self-supervised learning. In *Proceedings of the IEEE/CVF International Conference on Computer Vision*, pages 10181–10190, 2021.